The Plant Cell, Vol. 31: 1063–1076, May 2019, www.plantcell.org © 2019 ASPB.

Genetic Regulation of Ethylene Dosage for Cucumber Fruit Elongation[OPEN]

Tongxu Xin,[a,b,1] Zhen Zhang,[c,1] Shuai Li,[a] Shu Zhang,[a] Qing Li,[a] Zhong-Hua Zhang,[a] Sanwen Huang,[b] and Xueyong Yang[a,2]

[a] Key Laboratory of Biology and Genetic Improvement of Horticultural Crops of Ministry of Agriculture, Sino-Dutch Joint Lab of Horticultural Genomics, Institute of Vegetables and Flowers, Chinese Academy of Agricultural Sciences, Beijing 100081, China
[b] China Agricultural Genome Institute at Shenzhen, Chinese Academy of Agricultural Sciences, Shenzhen 518124, China
[c] College of Horticulture, Northwest A&F University, Yangling, Shaanxi 712100, China

ORCID IDs: 0000-0002-0318-8446 (T.X.); 0000-0002-4864-6180 (Z.Z.); 0000-0003-3728-007X (S.L.); 0000-0002-4478-0374 (S.Z.); 0000-0002-2397-5922 (Q.L.); 0000-0002-1034-227X (Z.-H.Z.); 0000-0002-8547-5309 (S.H.); 0000-0001-5894-9217 (X.Y.)

Plant organ growth and development are determined by a subtle balance between growth stimulation and inhibition. Fruit size and shape are important quality traits influencing yield and market value; however, the underlying mechanism regulating the balance of fruit growth to achieve final size and shape is not well understood. Here, we report a mechanistic model that governs cucumber (*Cucumis sativus*) fruit elongation through fine-tuning of ethylene homeostasis. We identified a cucumber mutant that bears short fruits owing to repressed cell division. *SF1* (*Short Fruit 1*) encodes a cucurbit-specific RING-type E3 ligase, and the mutation resulted in its enhanced self-ubiquitination and degradation, but accumulation of ACS2 (1-aminocyclopropane-1-carboxylate synthase 2), a rate-limiting enzyme for ethylene biosynthesis. The overproduction of ethylene contributes to the short-fruit phenotype of *sf1*. Dysfunction of ACS2 resulted in reduced ethylene production, but still repressed cell division and shorter fruit, suggesting that ethylene is still required for basal fruit elongation. SF1 ubiquitinates and degrades both itself and ACS2 to control ethylene synthesis for dose-dependent effect on cell division and fruit elongation. Our findings reveal the mechanism by which ethylene dosage is regulated for the control of cell division in developing fruit.

INTRODUCTION

Fruit, corresponding to the plant ovary, protects the developing seeds, and provides humans with a source of food and nutrition. Cucurbits are a large and diverse plant family that supply many important fruits (Bisognin, 2002). Cucurbit fruits develop from inferior ovaries and are well known for their extreme diversity in fruit size and shape (Grumet and Colle, 2016; Colle et al., 2017), which are also important agronomic traits for determining crop yield and external quality. Classic fruit morphogenesis is determined by four physiological phases of early development: ovary growth, fruit set, rapid cell division, and subsequent cell expansion (Grumet and Colle, 2016). However, the genetic and molecular basis in these developmental phases is largely unknown.

Plant organ growth is determined by a subtle balance between growth stimulation and inhibition, which confer optimal plasticity in response to endogenous or environmental cues. Cucurbit fruit development initiates with the formation of a female or bisexual flower, during which ethylene plays an essential role (Chen et al., 2016). The gaseous hormone ethylene coordinates numerous aspects of plant growth and responses to stress (Wen, 2014). The inhibition of cell expansion is a well-described ethylene response (Kieber et al., 1993). The role of ethylene in fruit development has recently been investigated. In tomato (*Solanum lycopersicum*), ethylene plays a role in suppressing fruit set in coordination with auxin and gibberellin (Shinozaki et al., 2015). In zucchini (*Cucurbita pepo*), exogenous application of ethylene inhibitors promotes parthenocarpic fruit growth (Martínez et al., 2013). Although ethylene is generally considered to inhibit growth, it also stimulates growth in specific tissues and cells or at low concentrations. For instance, in Arabidopsis (*Arabidopsis thaliana*), ethylene modulates the cell division and quiescence of stem cells in the roots (Ortega-Martínez et al., 2007). In cucumber (*Cucumis sativus*) seedlings, transient treatment with physiological concentrations of ethylene stimulates cell division and alters cell division polarity (Kazama et al., 2004). Therefore, the fine tuning of ethylene production in different tissues at different developmental phases is critical for plant development, influencing both the stimulation and repression of growth (Pierik et al., 2006). However, little is known about the genetic regulation of ethylene dosage for regulating the balance of fruit growth, and the mechanistic basis for the dose-dependent ethylene response remains speculative.

Here, we report that the RING-type E3 ligase short fruit 1 (SF1) regulates fruit cell division in cucumber by modulating ethylene dosage via ubiquitination and 26S proteasome-dependent degradation of both itself and 1-aminocyclopropane-1-carboxylate synthase 2 (ACS2). We showed dosage effects of ethylene on cell division and fruit elongation in cucumber using exogenous treatments involving a series of ethylene concentrations. The findings demonstrate a genetic basis of ethylene dose-dependent control for the balance of cell division in developing fruit.

[1] These authors contributed equally to this work.
[2] Address correspondence to yangxueyong@caas.cn.
The author responsible for distribution of materials integral to the findings presented in this article in accordance with the policy described in the Instructions for Authors (www.plantcell.org) is: Xueyong Yang (yangxueyong@caas.cn).
[OPEN]Articles can be viewed without a subscription.
www.plantcell.org/cgi/doi/10.1105/tpc.18.00957

IN A NUTSHELL

Background: Plant organ growth and development are determined by the subtle balance between growth stimulation and inhibition. Fruit size and shape are important quality traits influencing yield and market value. Cucurbits are a large and diverse plant family that supplies many important fruits. Cucurbit fruits develop from inferior ovaries and are known for their extreme diversity in size and shape—ranging from small to giant, and from oblate to elongate. However, the underlying mechanism regulating the balance of fruit growth to achieve final fruit size and shape is not well understood.

Question: What is the genetic and molecular basis for regulating the balance between cucumber (*Cucumis sativus*) fruit growth stimulation and inhibition?

Findings: Using two shortened fruit mutants, *sf1*, which exhibits reduced cell division and overproduces ethylene, and *acs2*, which exhibits reduced cell division but produces relatively little ethylene, we revealed the genetic and molecular mechanism controlling ethylene dosage for cucumber fruit elongation. We demonstrated the effects of different ethylene dosages on fruit elongation using ethylene gas as a direct ethylene treatment, providing major insight into the molecular basis of cucurbit fruit morphogenesis. Our findings may also provide a potentially useful method for generating a series of fruits with a gradient of lengths via physiological treatment or genome editing methods. Because fruit size preferences vary among consumer populations, this research could guide cucumber breeding practices.

Next steps: How do dose-dependent ethylene responses exert multiple roles in fruit cell division? Although the biphasic ethylene response model was proposed, the mechanistic basis for this diversification remains speculative. Cucumber fruit constitutes a potential important system for unravelling the signal transduction components involved in the different ethylene responses.

RESULTS

A Cucurbit-Specific RING-Type E3 Ligase

Using ethyl methanesulfonate mutagenesis, we identified a cucumber mutant bearing shortened fruits (*sf1*). Fruit morphogenesis was then characterized during early development stages (Figures 1A and 1B; Supplemental Figure 1A). We observed that the fruit length of the wild type (406 line) exhibits more rapid growth rate than that of the mutant (*sf1*) from 0 d after anthesis (DAA) to 8 DAA, whereas the fruit diameter does not significantly differ between the mutant and wild type (Supplemental Figures 1B and 1C). Considering that the average cell size of the *sf1* mutant was similar to that of the wild type along the longitudinal section (Figures 1C and 1D), we inferred that early cell division is repressed in *sf1*. Further investigation revealed no significant difference in cell number or cell size between the wild type and *sf1* along the transversal axis (Supplemental Figures 1D and 1E). However, on the longitudinal axis, although the average cell size was also identical (Figure 1E), the cell number was clearly lower in *sf1* (Figure 1F). The 8 DAA fruit of the *sf1* mutant contained nearly 50% fewer cells than did that of the wild-type plants (Figure 1F). These results indicate that the decreased fruit length associated with *sf1* results from reduced cell numbers along the longitudinal axis but not from cell expansion.

To genetically map the *sf1* locus, an F2 population was constructed by crossing *sf1* plants with wild-type plants. All F1 plants exhibited the same normal fruit-length phenotype as the wild-type plants. In the F2 population of 130 individuals, 23 plants displayed the short-fruit trait, whereas the remaining 107 plants were normal. The segregation pattern fit the Mendelian ratio of 3:1 ($\chi^2 = 3.70$, $P < 0.01$, *t* test, one tail), suggesting that *sf1* is a single recessive allele (Supplemental Table 1). To clone the candidate gene, whole-genome resequencing (> 10× coverage) of pooled genomic DNA samples from 20 short-fruit individuals (mutant pool) and 20 normal individuals (normal pool) from the F2 population was performed, and we identified 543 G-to-A (or C-to-T) single-nucleotide polymorphisms (SNPs) with a SNP index of > 0.7 between the two pools (Supplemental Data Set 1). We considered that the genomic region on chromosome 2 enriched with SNPs harbors the causal mutation for *sf1* (Figure 1G). Linkage analysis within the F2 population further delimited the *sf1* locus to a 1.2-Mb interval between SNP2G9169162 and SNP2G10364174, in which only SNP2G9983495 cosegregated with a short-fruit phenotype (Figure 1H). Within the interval, no other homozygous variants were discovered in the mutant pool. These results indicate that SNP2G9983495 is the causative mutation of the short-fruit phenotype.

SNP2G9983495 (G to A) is located within *Csa2G174140* (Figure 1I), which is annotated as encoding a putative RING-type E3 ligase, SF1. The G-to-A mutation results in an amino acid change from Arg (R) to Lys (K) at residue 230 (R230K). Alignment of the SF1 amino acid sequence with that of homologous proteins from various plant species showed that R-230 is conserved among land plants (Figure 1J). Phylogenetic analysis revealed that SF1 and its orthologs in melon and watermelon constitute a cucurbit-specific branch of the E3 ligase that belongs to the XB3 ortholog 4 in *Arabidopsis thaliana* (XBAT) family (Figure 1K; Supplemental Table 2; Supplemental Data Set 2; Nodzon et al., 2004).

To confirm that *SF1* is the causative gene genetically, clustered regularly interspaced short palindromic repeats (CRISPR)/CRISPR associated protein 9 (Cas9) was used to generate several *SF1*-edited plants, including two null mutants – one with a homozygous deletion of 4 bp and another with a homozygous deletion of 10 bp in the second exon of *SF1* (Supplemental Figures 2A

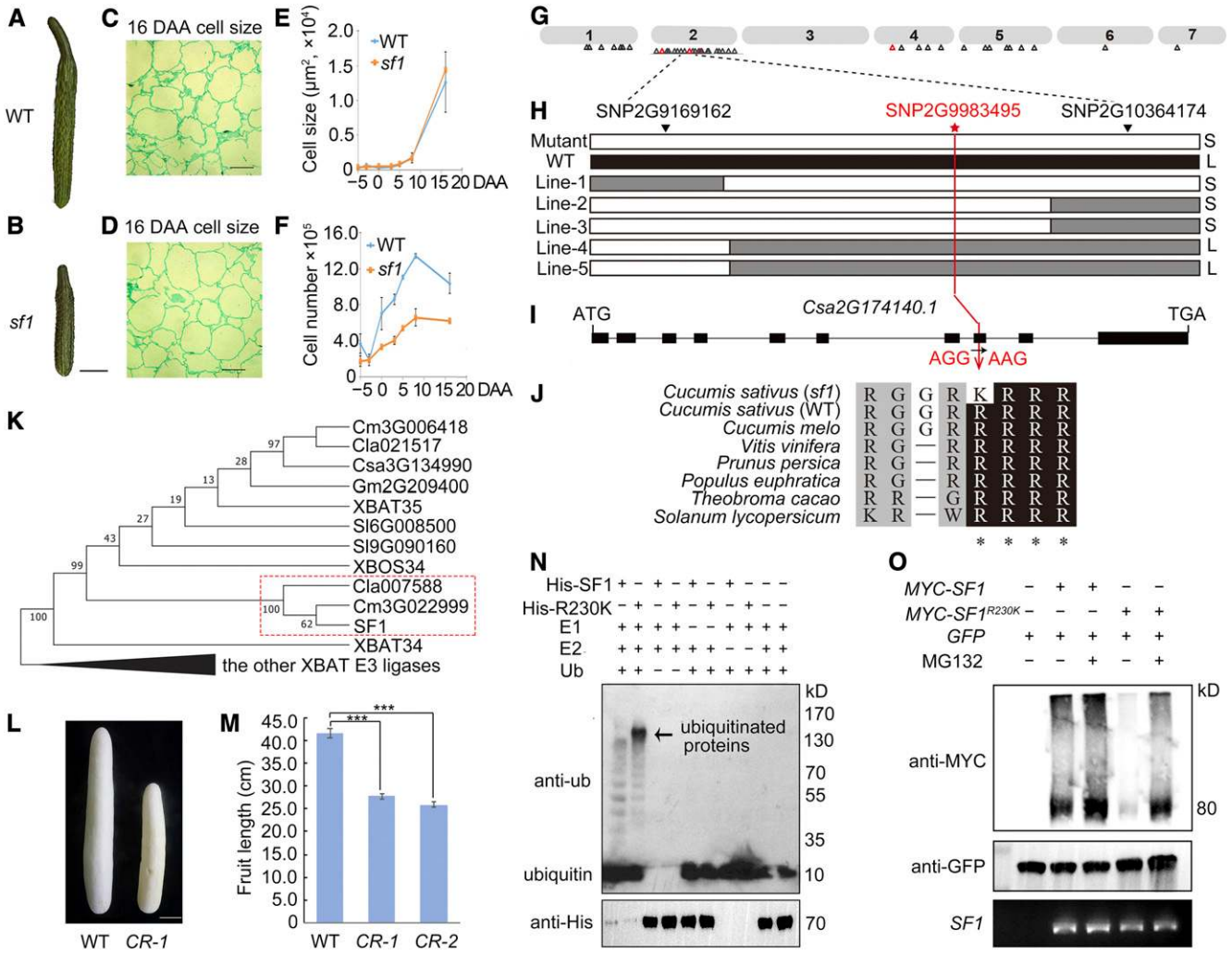

Figure 1. Characterization and Identification of *SF1*.

(A) and **(B)** When compared with wild type (WT; **A**), *sf1* **(B)** bears short fruit. Scale bar = 5 cm.
(C) and **(D)** Mesocarp cells of wild type **(C)** and *sf1* **(D)** at 16 DAA along a longitudinal section. Scale bar = 50 μm.
(E) The average cell size shows no significant difference between wild type and *sf1*. Bars = means from three independent fruits ± SEM.
(F) The cell proliferation rate is substantially arrested in the *sf1* fruit compared with wild type along a longitudinal axis. Bars = means from three independent fruits ± SEM.
(G) Genomic distribution of homozygous SNPs. Hollow triangles indicate SNPs.
(H) Linkage analysis of the F2 population using dCAPS markers. The red star indicates the only SNP cosegregating with the short fruit phenotype.
(I) Gene structure of *Csa2G174140*.
(J) Alignment of *Csa2G174140* homologs from diverse species.
(K) SF1 is a cucurbit-specific branch of an XBAT-related E3 ligase.
(L) and **(M)** Both the *SF1* null-mutant plants *CR-1* and *CR-2* displayed significantly decreased fruit length. Bars = means of three fruits from three independent plants ± SEM. Scale bar = 5 cm. *** $P < 0.01$ (*t* test, one tail).
(N) In vitro ubiquitination reactions. Those proteins were purified from *E. coli* extracts; (+) and (−), respectively, represent participation and absence in the reaction. Proteins were separated by standard SDS-PAGE and analyzed by immunoblotting using anti-ubi and anti-His. Arrows indicate the ubiquitinated proteins.
(O) Agroinfiltration expression in *Nicotiana benthamiana* was performed to confirm the self-ubiquitination ability of CsSF1 in vivo. The (+) and (−), respectively, represent participation and absence in the reaction. The SF1 mRNA expression levels and the GFP protein amount that were detected as internal controls remained consistent across all lanes.

and 2B). Both the *SF1* null-mutant plants *CR-1* (*CRISPR-line 1*) and *CR-2* displayed a 40% reduction in fruit length (Figures 1L and 1M), which was consistent with the short-fruit phenotype of *sf1*. Thus, *Csa2G174140* is responsible for the observed short-fruit phenotype.

To determine the mRNA expression pattern of *SF1*, the number of fragments per kilobase of transcript per million mapped reads from the RNA sequencing (RNA-seq) data of different cucumber tissues was assessed. *SF1* mRNA was expressed ubiquitously (Supplemental Figure 3A). To determine SF1 protein expression, rabbit polyclonal antibodies for SF1 were raised against synthetic peptides, and the antibody specificity was confirmed (Supplemental Figures 3B and 3C). Interestingly, SF1 was detected only in 0 DAA fruit and stem (Supplemental Figure 3D), suggesting a posttranslational regulation of SF1.

To investigate whether CsSF1 is a functional E3 ligase and whether the R230K mutation affects its activity, the His-tagged or glutathione *S*-transferase (GST)-tagged recombinant SF1, Ubiquitin conjugating enzyme 2 (E2), and Ubiquitin conjugating enzyme 8, the AtUBC8 homolog (CsUBC8) were purified from *Escherichia coli* extracts (Supplemental Figure 4A) and used for in vitro ubiquitination reactions. The results showed that CsSF1 can self-ubiquitinate. A polyubiquitination signal was observed by immunoblotting with an anti-ubiquitin antibody (Figure 1N). As negative controls, no polyubiquitination of CsSF1 was detected when E1, E2, ubiquitin, or His-CsSF1 was excluded from the reaction (Figure 1N). Unexpectedly, self-ubiquitination appeared to be enhanced by the R230K mutation (Figure 1N). Because E3 ubiquitin ligase is usually activated by dimerization, we also investigated the capacity of CsSF1 to self-interact, showing that both CsSF1 and the CsSF1^{R230K} proteins could homodimerize (Supplemental Figure 4B). To confirm the self-ubiquitination ability of CsSF1 in vivo, we performed agroinfiltration expression in *Nicotiana benthamiana* and observed that SF1^{R230K} was easier to degrade than was SF1 and that the degradation could be repressed by MG132, a 26S proteasome inhibitor (Figure 1O). The *SF1* mRNA expression levels and the green fluorescent protein (GFP) amount that were detected as internal controls remained consistent across all lanes (Figure 1O). Together, these results demonstrated that SF1 encodes a functional cucurbit-specific RING-type E3 ligase and that the R230K mutation results in its enhanced self-ubiquitination and degradation by the 26S proteasome, indicating that *sf1* is a loss-of-function mutant.

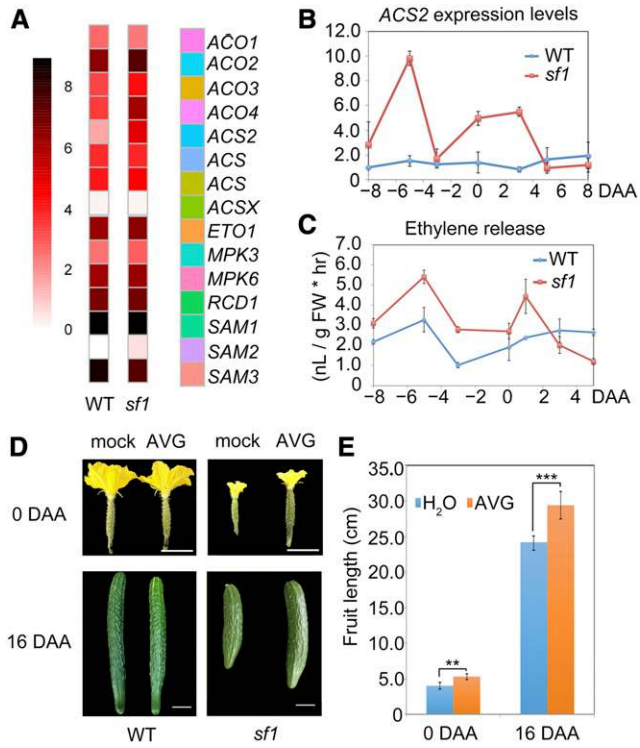

Figure 2. The Short-Fruit Phenotype of *sf1* Results from Increased Production of Ethylene.

(A) The genes controlling ethylene production are enriched in the upregulated gene set in 0 DAA fruits of *sf1*, showing *ACS2* expression was significantly increased. Scaled log2 expression values are shown. SAM, *S*-adenosyl-L-methionine; ACO, ACC oxidase; MPK, Mitogen-activated protein kinases; RCD, Radical-induced cell death.

(B) *ACS2* expression levels in fruits were upregulated in *sf1* during early development. Bars = means from three independent pools of fruits ± SEM.

(C) The ethylene production was elevated in *sf1* fruits during early fruit growth. FW, Fresh Weight. Bars = means of three fruits from three independent plants ± SEM.

(D) and **(E)** A 1-mM AVG treatment partially complemented the short fruit phenotype of *sf1*, but had no effect on wild type (WT). Scale bar = 4 cm. **P < 0.05; ***P < 0.01 (*t* test, one tail). Bars = means of three fruits from three independent plants ± SEM.

Overproduction of Ethylene in *sf1*

To further understand the molecular mechanism by which SF1 contributes to rapid fruit cell division, we examined the genome-wide gene expression in fruit cells at 0 DAA in *sf1* and wild-type plants. A total of 904 genes were significantly differentially expressed (> 1.5-fold or < 0.67-fold; P < 0.05), including 523 and 381 genes that were up- and downregulated, respectively, in *sf1* fruit (Supplemental Data Set 3). Interestingly, we found that a group of genes involved in ethylene production, such as the genes encoding aminocyclopropane-1-carboxylic acid synthase (ACC synthase, ACS), ACC oxidase, and *S*-adenosyl-L-methionine, are enriched in the upregulated gene set (Figure 2A). *ACS2*, which encodes 1-aminoacyclopropane-1-carboxylic acid synthase, is an important gene that determines bisexual flower formation in cucumber, and its expression was significantly upregulated by 7-fold in *sf1* (Figure 2A; Supplemental Data Set 3). We next determined that *ACS2* expression levels were higher in the *sf1* plants than in the wild-type plants during early fruit development (Figure 2B). As ACS proteins catalyze the rate-limiting step in ethylene synthesis, with the exception of 3 and 5 DAA, the ethylene production of the *sf1* fruits was ~50% greater than that of the wild-type fruits during the early fruit growth stage (Figure 2C).

To determine whether the short-fruit phenotype of *sf1* results from increased production of ethylene, we attempted to test whether the phenotype could be rescued by the ethylene synthetic inhibitor 1-aminoethoxyvinyl glycine (AVG). A concentration of 1 mM AVG partially rescued the short-fruit phenotype, but had

no significant effect on wild type, indicating that the increased ethylene is essential for the short-fruit phenotype of the *sf1* mutant (Figures 2D and 2E).

To confirm the role of ethylene signaling in fruit elongation, we used 1-methylcyclopropene to block ethylene perception in *sf1*. Treatment with 1-methylcyclopropene at different concentrations (0, 1.0, 2.0, and 3.0 ppm) produced dose-dependent effects on the length of *sf1* fruits (Supplemental Figure 5). The 1.0-ppm treatment partially complemented the short-fruit phenotype (Supplemental Figures 6A and 6B). These results further indicate that the short-fruit phenotype of the *sf1* mutant is due to the increased ethylene perception.

The Short-Fruit Mutant *acs2*

We previously cloned *ACS2* (*Csa1G580750*) that controls bisexual expression (Li et al., 2009). To further dissect the relationship between *SF1* and *ACS2*, we investigated the cucumber mutant *acs2* (line 83H), in which *ACS2* harbors a single-point mutation at the 33rd amino acid residue (Gly [G] to Cys [C]; G33C), partially abolishing the ACS enzyme activity (Li et al., 2009; Supplemental Figure 7A). In addition to the floral sex phenotype, *asc2* plants also bear shorter fruits than do wild-type plants (83G, the near-isogenic line of 83H; Figure 3A; Supplemental Figures 7B and 7C). We also determined that the repressed fruit elongation resulted from a reduced cell number along the longitudinal axis rather than from cell expansion (Figures 3B and 3C); moreover, the ethylene release in *acs2* fruit was significantly reduced ($P < 0.05$; Figure 3D). To confirm the role of *ACS2* in fruit development, CRISPR-Cas9 was used to generate several ACS2-edited plants, including two null mutants – one with a homozygous deletion of 1 bp and another with a homozygous deletion of 76 bp (17 bp plus 59 bp; Supplemental Figure 7D). Both cucumber *ACS2* knock-out mutants displayed androecy in plants that bore only male flowers (Supplemental Figure 7E), indicating the essential role of ACS2 in cucumber fruit formation.

To determine the ACS2 protein expression pattern, rabbit polyclonal antibodies of ACS2 were raised against specific synthetic peptides (Supplemental Figure 8A), and the antibody specificity was confirmed (Supplemental Figure 8B). We observed that the G33C mutation in *acs2* significantly affects the accumulation of ACS2 (Supplemental Figure 8B), indicating that the decreased enzyme activity of $ACS2^{G33C}$ downregulates its expression in a positive feedback manner, in agreement with a previous report (Li et al., 2012). The results also demonstrated that *acs2* is a loss-of-function mutant. We further observed that, in wild-type fruits, in contrast with the stable mRNA expression patterns (Figure 3E), ACS2 protein was preferentially accumulated in fruit tissues (Supplemental Figure 8C); moreover, its protein levels increased from −8 to −5 DAA, and then decreased after 3 DAA (Figure 3F). These results suggest a posttranslational regulation of ACS2, which supports ACS2 being a potential substrate of SF1 for fruit length regulation.

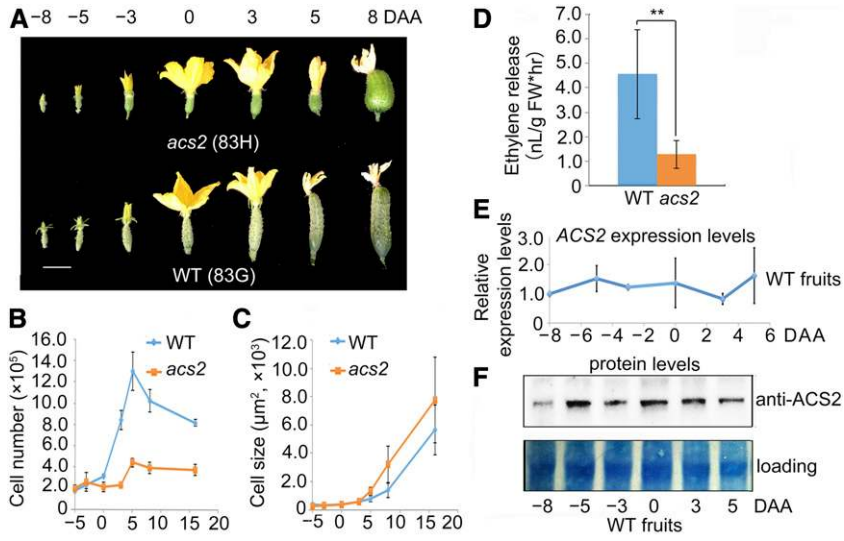

Figure 3. The Short-Fruit Mutant *acs2* Produces Less Ethylene Than Does Wild Type (WT).

(A) Wild-type (83G) and *acs2* (83H) fruits during early fruit development. Scale bar = 3 cm.

(B) Decrease of cell number in *acs2* fruit compared with that in wild type along the longitudinal axis. Bars = means from three independent fruits ± SEM.

(C) The average cell size shows no significant difference between wild type and *acs2*. Bars = means from three independent fruits ± SEM.

(D) The ethylene release was significantly reduced in 0 DAA fruits of *acs2*. FW, Fresh Weight. Bars = means of three fruits from three independent plants ± SEM. **$P < 0.05$ (*t* test, one tail).

(E) The mRNA expression levels during early fruit development in wild-type fruits. Bars = means of three independent pools of fruits from three independent plants ± SEM.

(F) The protein expression of ACS2 in wild-type fruits increased significantly from −5 to 3 DAA. Proteins were analyzed by immunoblotting using anti-ACS2. Coomassie brilliant blue (Coomassie) staining of the bottom part of each blot is shown as a loading control.

Interaction between SF1 and ACS2

To confirm that ACS2 is a ubiquitinated substrate of SF1 for proteasomal degradation, we first determined their interaction in vitro and in vivo. For yeast two-hybrid assays, the RING domain of SF1 and SF1^{R230K} was made nonfunctional by mutating two essential zinc ligand residues, Cys-336 and His-338, to Ala (SF1-AA and SF1^{R230K}-AA) to prevent the ubiquitination and degradation of itself (Nodzon et al., 2004). Both SF1-AA and SF1^{R230K}-AA could interact with ACS2 to induce *Trp1*, *Leu2*, *His3*, *Ade2*, and LacZ reporter genes in AH109 yeast lines (Figure 4A).

The specific interaction between SF1 and ACS2 in vitro was verified via GST pull-down assays. We observed that Myelocytomatosis (MYC)-ACS2 interacted with GST-SF1 and GST-SF1^{R230K}, whereas no interaction signals were observed when GST protein was used as a control (Figure 4B). To obtain evidence of the SF1 and ACS2 interaction in vivo, we performed coimmunoprecipitation. The pairwise FLAG-ACS2/MYC-SF1 or FLAG-ACS2/MYC-SF1^{R230K} agrobacteria were transiently expressed in *N. benthamiana* leaves supplemented with MG132. FLAG-ACS2 formed a protein complex with MYC-SF1 and MYC-SF1^{R230K} (Figure 4C). All of these results demonstrate that SF1 specifically interacts with ACS2.

Ubiquitination and Degradation of ACS2 by SF1

To examine the possibility that SF1 mediates the direct ubiquitination of ACS2, we performed in vitro ubiquitination assays using recombinant proteins. ACS2 was found to be effectively ubiquitinated by SF1 and SF1^{R230K} in the presence of ubiquitin (Figure 5A). There was no perceivable difference between the ubiquitination ability of SF1 or SF1^{R230K}. Moreover, as the ratio of GST-SF1:ACS2 or GST-SF1^{R230K}:ACS2 increased from 1 to 10, the intensity of the ubiquitinated bands gradually increased; however, when the ratio reached 60, the ubiquitination of ACS2 was repressed, indicating that SF1 catalyzes the ubiquitination of ACS2 in a dose-dependent manner (Figure 5A).

We then used a cell-free degradation assay to monitor the turnover of the enzyme in the presence and absence of MG132 in vitro. In the absence of MG132, His-MYC-ACS2 gradually disappeared when incubated with protein extracts from wild-type fruits, and the degradation rate of His-MYC-ACS2 protein decreased when incubated with protein extracts from *sf1* fruits. This degradation can be blocked by MG132 (Supplemental Figures 9A and 9B). Thus, ACS2 can be degraded by SF1 via 26S proteasomes.

To further confirm that the SF1-mediated ubiquitination of ACS2 promotes protein degradation in vivo, we transiently expressed FLAG-ACS2, MYC-SF1, MYC-SF1^{R230K}, and a GFP internal

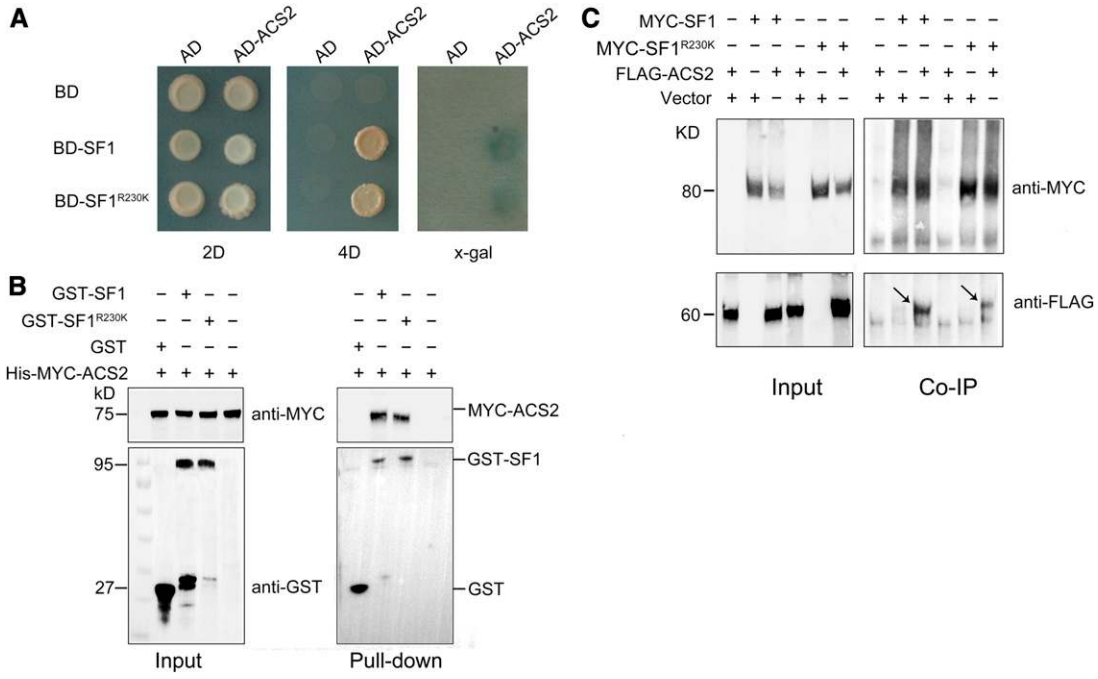

Figure 4. SF1 Interacts With ACS2.

(A) Interaction between SF1 and ACS2 verified by yeast two-hybrid assays. Interaction between SF1 and ACS2 was identified, showing growth on medium lacking Leu, Try, His, and Ade (4D), and showing blue color in an X-Gal assay. BD, Binding domain; AD, Activation domain; 2D, SD-Leu-Trp; 4D, SD-Ade-Leu-Trp-His; X-gal, bromochloroindoxyl galactoside.

(B) Pull-down assays confirming the interaction between GST-SF1 or GST-SF1^{R230K} and His-MYC-ACS2 in vitro. GST protein was used as the negative control.

(C) Coimmunoprecipitation assays indicating the interaction between SF1 and ACS2 in vivo. Arrows indicate the immunoprecipitated FLAG-ACS2 by MYC-SF1 and MYC-SF1^{R230K}. The (+) and (−) represent participation and absence, respectively, in the reaction.

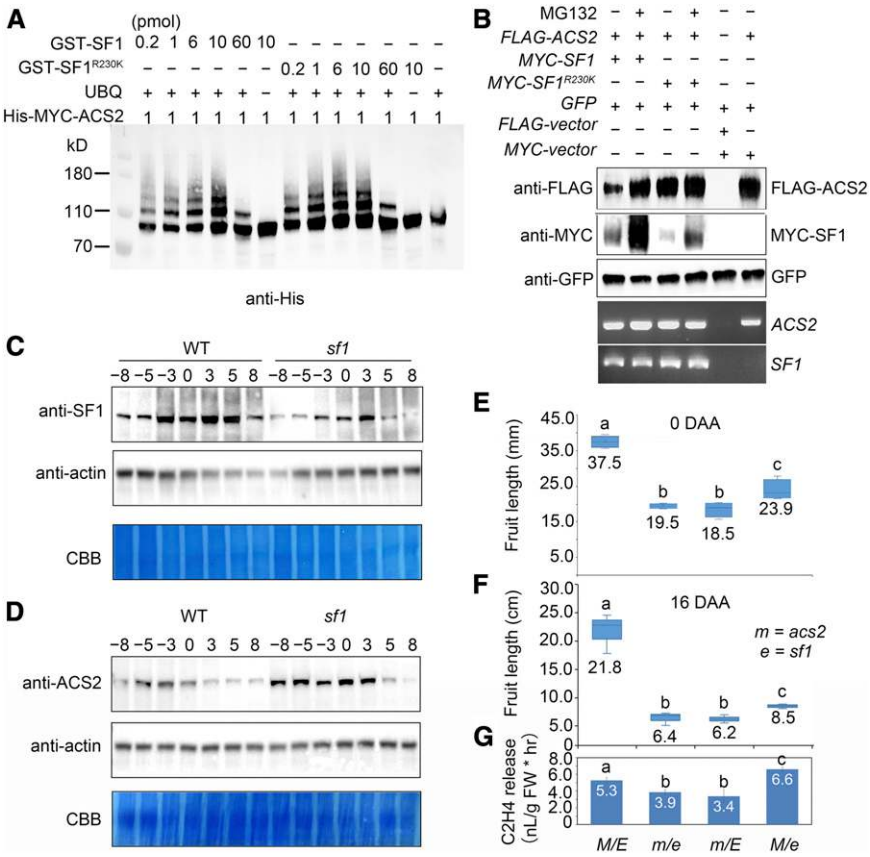

Figure 5. ACS2 is a Substrate of SF1.

(A) Ubiquitination of ACS2 by SF1 in vitro. The above two lines of numbers represent the concentration of GST-SF1 and GST-SF1^{R230K}. Reaction were analyzed by immunoblotting using anti-His.

(B) SF1 promotes ACS2 degradation via 26S proteasomes. When ACS2 and SF1^{R230K} were coexpressed, the dramatic degradation of SF1^{R230K} proteins resulted in a significant accumulation of ACS2. SF1 and ACS2 were expressed in *N. benthamiana* leaves treated with (+) or without (−) MG132. GFP was used as the control for the infiltration event. Bottom panels, RNA levels of *ACS2* and *SF1*.

(C) and **(D)** Expression profiles of SF1 **(C)** and ACS2 proteins **(D)** in wild-type (WT) and *sf1* fruit during early fruit development, showing decreased SF1 protein levels while increased ACS2 protein levels in *sf1*. Actin was used as an internal control. Coomassie brilliant blue (CBB) staining of the bottom part of each blot is shown as a loading control.

(E) and **(F)** Boxplots show the epistasis of *acs2* (*m*) to *sf1* (*e*) genetically. Twenty fruits of each genotype at 0 DAA and 16 DAA are shown: wild type (*M E*), *m e*, *m E*, and *M e* fruit from 20 independent plants were identified to measure fruit length. Bars = means ± SEM ($n = 20$). Different lowercase letters indicate significant difference, $P < 0.05$, Tukey's test.

(G) The ethylene release in wild type (*M E*), *m e*, *m E*, and *M e* fruits at 0 DAA, showing that *m E* and *m e* fruits produced relatively less ethylene, and *M e* fruits produced more ethylene than in wild type. FW: Fresh Weight. Bars = means from three independent fruits ± SEM. Different lowercase letter indicates significant difference, $P < 0.01$, Tukey's test.

control protein by agroinfiltration in *N. benthamiana* (Figure 5B). We assessed the *ACS2* and *SF1* mRNA expression levels and the GFP internal control protein levels to determine whether they remained consistent in related lanes. When compared with the separate infiltration of FLAG-ACS2, coexpression of FLAG-ACS2 and MYC-SF1 in the same leaf region resulted in significant degradation of FLAG-ACS2. When MG132 was infiltrated into the same area, the degradation of both FLAG-ACS2 and MYC-SF1 was repressed (Figure 5B), indicating that SF1 targets ACS2 for ubiquitin-dependent degradation by the 26S proteasome. Intriguingly, when FLAG-ACS2 and MYC-SF1^{R230K} were coexpressed, the SF1^{R230K} proteins were substantially self-degraded, resulting in a significant accumulation of FLAG-ACS2 (Figure 5B). To confirm the above results in planta, total protein extracts from fruits were prepared for immunoblotting. The overall amount of SF1^{R230K} protein was decreased during fruit development in *sf1* (Figure 5C), which is consistent with the transient expression results from *N. benthamiana* (Figures 1O and 5B). It was further demonstrated ACS2 indeed accumulated to a greater extent in the *sf1* fruits than in the wild-type fruits (Figure 5D), which explained our previous observation that ethylene was overproduced in *sf1* fruits (Figure 2C).

The above results demonstrated that SF1 and ACS2 interact biochemically. Because the genetic backgrounds of *sf1* (East

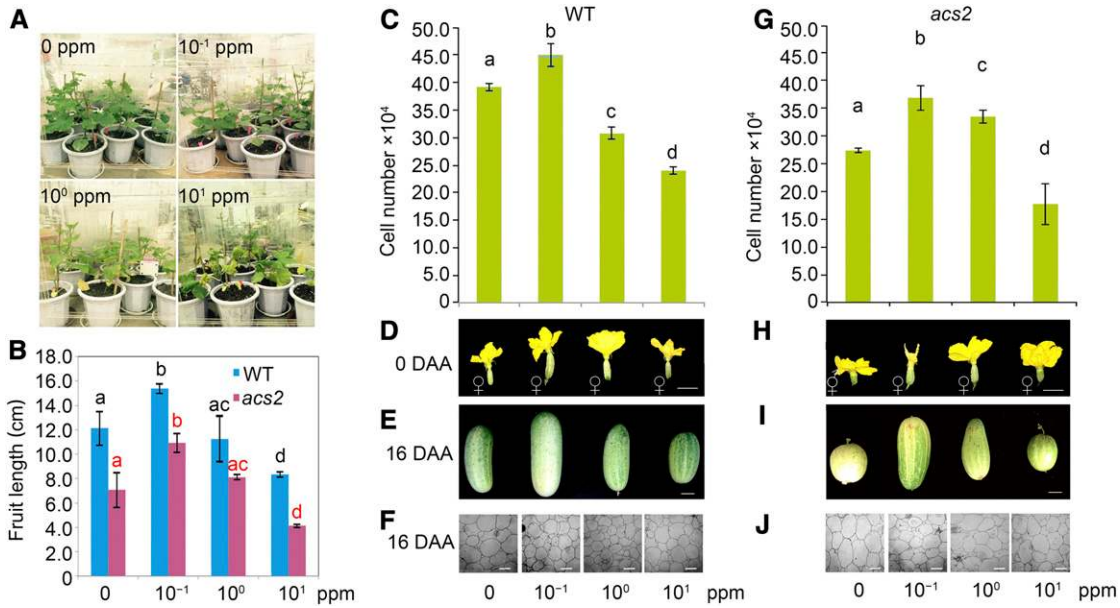

Figure 6. Ethylene Dose-Dependent Effects on Cucumber Fruit Elongation.

(A) Exogenous ethylene treatment for wild type (WT) and *acs2* at different concentrations of ethylene for 1 week in four acrylic boxes. Four different concentrations of ethylene in four boxes are shown.

(B) The 16 DAA fruit length of wild type and *acs2* treated with different concentrations of ethylene. Bars = means of three fruits from three independent plants ± SEM. Different lowercase letters indicate significant difference, $P < 0.01$, Tukey's test.

(C) Cell number of 0 DAA fruits of wild type treated with different concentrations of ethylene. Bars are means of three fruits from three independent plants ± SEM. Different lowercase letter indicate significant difference, $P < 0.01$, Tukey's test.

(D) to (F) Phenotypes of 0 DAA **(D)** and 16 DAA **(E)** fruits of wild-type plants treated with different concentrations of ethylene. Scale bar = 2 cm. **(F)** Mesocarp cells of wild type at 16 DAA. Scale bar = 50 μm.

(G) Cell number of 0 DAA *acs2* fruits treated with different concentrations of ethylene. Bars = means of three fruits from three independent plants ± SEM. Different lowercase letters indicate significant difference, $P < 0.01$, Tukey's test.

(H) to (J) Phenotypes of 0 DAA **(H)** and 16 DAA **(I)** *acs2* fruits treated with different concentrations of ethylene. Scale bar = 2 cm. **(J)** Mesocarp cells of *acs2* at 16 DAA. Scale bar = 50 μm.

Asian background) and *acs2* (Eurasian background) are distinct, to confirm that *SF1* and *ACS2* interact genetically, we developed a series of BC_2S_1 lines using 1983H (*acs2*) as the donor and line 406 as the recurrent parent (*sf1* and wild type, each for backcrossing once). Plants with a genotype of *M E* (wild type, *ACS2/SF1*), *m E* (*acs2*), *m e* (*acs2/sf1*), or *M e* (*sf1*) were identified as the near-isogenic lines for measuring the fruit length and ethylene release (Supplemental Figure 10). The phenotypic analysis revealed that, when compared with the other plants, the wild-type (*M E*) plants produced longer fruits, and the fruits of *M e* plants were significantly shorter. The length of the *m E* fruits was reduced the most, whereas the fruit length of the *m e* double mutant was similar to that of *m E* but not similar to that of the synthetic *m* plus *e* (Figures 5E and 5F; Supplemental Figure 10). These results indicate that *acs2* (*m*) is genetically epistatic to *sf1* (*e*). The ethylene release in 0 DAA fruits of *M E* (wild type), *m E*, *m e*, and *M e* was consistent with the observation on *acs2* and *sf1* mutants. Thus, *m E* and *m e* produced relatively less ethylene, and *M e* produced more ethylene than the wild type. By contrast, the difference in ethylene release between *m E* and *m e* is not significant (Figure 5G). As in the double mutant *m e*, the mutation of E3 ligase activity in *sf1* that results in an increase in ACS2 protein cannot overcome the reduction in ethylene biosynthetic activity in the *acs2* mutant, further demonstrating the epistasis of *acs2*.

Together, the above results demonstrate that SF1 targets both itself and ACS2 for ubiquitin-dependent degradation to regulate both the ethylene dosage and balance of cell division in cucumber fruit.

Ethylene Dose-Dependent Fruit Elongation

When compared with wild-type plants, *sf1* plants bear shorter fruits due to the overproduction of ethylene, whereas *acs2* plants produce less ethylene but also bear shorter fruits. These lines of evidence suggest that the tight control of ethylene production is responsible for cucumber fruit elongation.

To assess this possibility, 1-month-old wild-type and *acs2* cucumber plants were transferred into four acrylic chambers, with five plants of wild type and five plants of *acs2* in each chamber (Wen, 2014). The four boxes were treated with different concentrations of ethylene (0, 10^{-1}, 10°, and 10^1 ppm) for 1 week (Figure 6A). The ethylene treatment exerted a dose-dependent effect on fruit elongation for the wild-type and *acs2* plants. Under 10^{-1} ppm ethylene, the *acs2* fruit length significantly recovered, but the effect was diminished when 10° ppm ethylene was

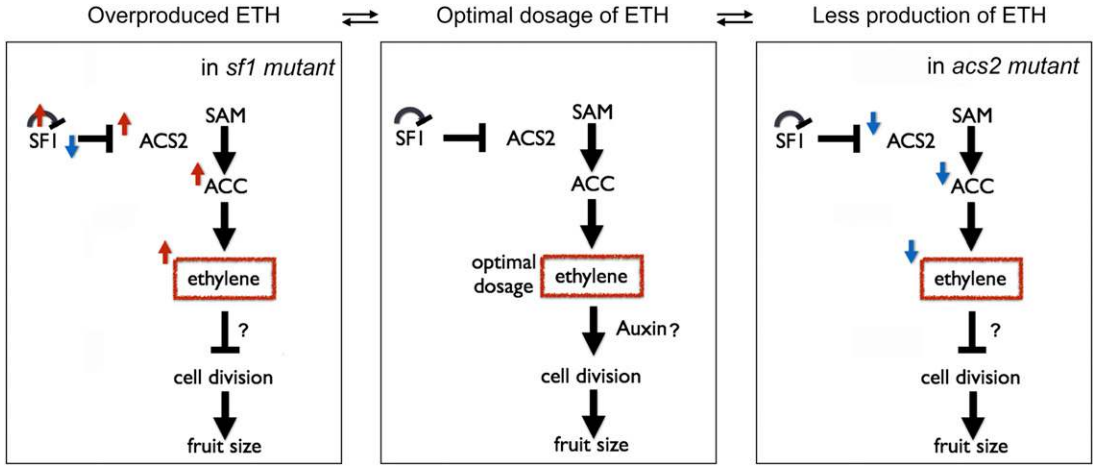

Figure 7. Regulatory Mechanism of Ethylene Dosage for Cell Division in Developing Cucumber Fruit.

SF1 regulates the ethylene dosage by targeting both itself and ACS2 for ubiquitin-dependent degradation. The ethylene biphasic response regulates the balance of cell division and fruit growth. Ethylene is highlighted in red rectangles. Black arrows and bar-ended lines represent positive and negative interactions, respectively. Red and blue arrows represent activation and repression, respectively. ETH, ethylene; SAM, *S*-adenosyl-L-methionine.

applied; however, under 10^{1} ppm ethylene, the *acs2* fruit length was significantly lower (Figure 6B). The same dose-dependent effect of ethylene on fruit elongation was also observed for the wild-type fruits (Figure 6B).

To confirm that the ethylene dose-dependent effect on fruit length is due to changes in cell division, we compared the mesocarp cell number between wild type (Figures 6C to 6F) and *acs2* (Figures 6G to 6J) along the longitudinal axis using 0 DAA fruits under different ethylene concentrations. Although cell size was reduced to a certain degree in response to ethylene treatment, the number of cells increased under the relatively low ethylene doses (10^{-1} ppm for wild type and 10^{-1} and 10° ppm for *acs2*) but decreased under higher ethylene concentrations. We also observed that sex of the flowers produced of the *acs2* mutant plants changed from bisexual to female flowers when treated with continuously increasing concentrations of ethylene; however, the effect of ethylene on sex expression is not dependent on the dose of ethylene (Figure 6H). Together, our findings provide genetic and molecular evidence that SF1 ubiquitinates and degrades both itself and ACS2 to tightly control ethylene synthesis for dose-dependent cell division and fruit elongation in cucumber (Figure 7).

DISCUSSION

Plant hormones are key factors required for plant growth, and among them, ethylene plays essential roles in various plant developmental processes, both by stimulating and inhibiting growth (Vandenbussche et al., 2012). In this study, cucumber fruit constituted an attractive system for understanding the dose-dependent control of the subtle balance of cell division by ethylene.

Ethylene contributes to the control of the flower sex type of cucurbit plants (Rudich et al., 1969). ACS catalyzes the rate-limiting step in ethylene biosynthesis, producing ACC from S-adenosylmethionine (Adams and Yang, 1979; Yang and Hoffman, 1984). Dysfunction of CsACS2 and CmACS7 in cucumber and melon (*Cucumis melo*) leads to the development of hermaphroditic flowers (Boualem et al., 2015), whereas bisexual flowers are associated with round-fruit phenotypes (Liu et al., 2008; Monforte et al., 2014), suggesting that ethylene promotes cucurbit fruit elongation.

Ethylene has long been recognized as a growth inhibitor; however, evidence is accumulating that ethylene can also promote growth depending on endogenous and environmental conditions and plant developmental stage (Dugardeyn and Van Der Straeten, 2008). The application of ethylene to dark-grown seedlings inhibits hypocotyl elongation (Guzmán and Ecker, 1990); this growth inhibition is caused by a decrease in cell elongation (Le et al., 2005). Under low nutrient conditions, low concentrations of ethylene treatment increase hypocotyl growth (Smalle et al., 1997) by stimulating additional cortex cell division but not cell elongation (Saibo et al., 2003). Studies suggest that auxin transport (Vandenbussche et al., 2003) or brassinosteroid signaling (De Grauwe et al., 2005) is involved in ethylene-mediated hypocotyl elongation. Recent studies on tomato and zucchini fruits showed that ethylene suppresses fruit set; however, those studies used ACC or ethephon for treatment. ACC and ethephon treatments may not accurately reproduce natural ethylene responses in some physiological processes (Zhang and Wen, 2010).

Although numerous quantitative trait loci for fruit length and shape in cucurbit plants have been identified (Qi et al., 2013; Wei et al., 2014; Bo et al., 2015; Weng et al., 2015; Pan et al., 2017), the genetic and molecular basis of these traits remain largely unknown. In the current study, using two shortened fruit mutants, *sf1*, which exhibits reduced cell division and overproduces ethylene, and *acs2*, which exhibits reduced cell division but produces relatively less ethylene, we revealed the genetic and molecular control of ethylene dosage for cucumber fruit elongation. We demonstrated the effects of different ethylene dosage on fruit elongation using ethylene gas as a direct ethylene treatment, providing major insight into the molecular basis of cucurbit fruit

morphogenesis. Cell size was increased in *acs2* fruits along the transversal axis (Supplemental Figure 11), and the suppression effect of ethylene on diameter appears to be different from the dose-dependent effect on length, suggesting the complex and pleiotropic effects of ethylene on cell division rate, cell division polarity, and cell expansion. Our findings may also provide a potentially useful method to generate a series of fruits with a gradient of lengths via physiological treatment or genome editing methods. Because fruit size preferences vary among consumer populations, this research could guide cucumber breeding practices.

ACS catalyzes the rate-limiting step in ethylene biosynthesis, and the amount of ACS2 protein is positively associated with ethylene production (Wen, 2014). The stability of individual ACS proteins is tightly regulated by phosphorylation, dephosphorylation, and ubiquitination-mediated proteasomal degradation (Wen, 2014), which is critical for fine tuning ethylene biosynthesis in response to various endogenous and environmental signals (Pierik et al., 2006). In Arabidopsis, the ethylene-overproducer with constituent of ubiquitin ligase 3 E3 Ligase complex targets AtACS5 and AtACS9 for degradation by the 26S proteasome (Wang et al., 2004); the RING-type E3 ligase AtXBAT32 targets AtACS7 for proteasomal degradation to regulate lateral root production (Prasad et al., 2010; Lyzenga et al., 2012). In this study, the control of ethylene doses for cucumber fruit elongation was achieved through the posttranslational degradation of ACS2 by the RING-type E3 ligase SF1 via the 26S proteasome pathway. In melon, the mutation of CmACS7 is reported to be associated with round fruit (Monforte et al., 2014; Boualem et al., 2015), suggesting that a conserved regulatory mechanism underlying ethylene dose-dependent fruit elongation exists in cucurbit plants.

The ethylene dose-dependent response has been reported for some species and tissues (Pierik et al., 2006). For example, in *N. benthamiana*, petiole growth and stem elongation were stimulated at low ethylene concentrations, and repressed at higher ethylene concentrations (Pierik et al., 2003, 2004). How do dose-dependent ethylene responses exert multiple roles in fruit cell division? Although the mechanistic basis for this diversification remains speculative, the biphasic ethylene response model was proposed. It is inferred that the interactions between ethylene and other signal transduction components might dependent on specific ethylene concentration, and the signal transduction pathways that stimulate growth are probably different to those that inhibit growth (Pierik et al., 2006). Cucumber fruit constitutes a potential important system for unraveling the signal transduction components involved in the different ethylene responses.

METHODS

Plant Material

The seeds of cucumber (*Cucumis sativus*) inbred line 406 (North China type) were treated with 1% (v/v) ethyl methanesulfonate (Sigma Aldrich) in mutagenesis experiments. The M1 plants were self-pollinated, and the short fruit line *sf1* was identified in the M2 population. Then, *sf1* was crossed with the wild-type 406, and an F2 population was derived from self-crossed F1 plants. The near-isogenic lines 1983G and 1983H (Liu et al., 2008) were used in this study. The cucumber inbred line CU2 was used in cucumber transformation. All cucumber plants were cultivated in the greenhouse at day/night temperatures of 24/18°C with a light regime of 16-h natural light/8-h dark in the Chinese Academy of Agricultural Sciences. Standard management was performed during cultivation.

The *Nicotiana benthamiana* plants were cultivated in pots in a growth chamber with a light regime of 16-h light/8-h dark at 22°C.

Derived Cleaved-Amplified Polymorphic Sequence Markers

For fine mapping of *sf1*, we developed derived cleaved-amplified polymorphic sequence (dCAPS) markers (Neff et al., 1998) on chromosome 2. The primers for dCAPS markers used to verify the SNP were designed by the web-based software dCAPS FINDER 2.0. PCR products, which were digested with appropriate restriction enzymes (Supplemental Table 3), were subsequently separated by electrophoresis on 8% (w/v) polyacrylamide gels.

Measurement of the Cell Number and Size

To measure the cell size and number of fruits of 406, *sf1*, 1983G, and 1983H, sliced samples from different periods at −5, −3, 0, 3, 5, 8, and 16 DAA were fixed in the solution of 70% (v/v) ethanol, acetic acid, and formaldehyde (90:5:5 by volume). Five-millimeter-thick slices cut from different parts of the cucumber fruit (outer, middle, and inner pericarp) were embedded in paraffin. Then, 8-μm-thick sections were prepared from both cross-sections and longitudinal direction with a microtome and stained with hematoxylin-eosin. Subsequently, these sections were imaged using a microscope (OLYMPUS BX51). The cell number and cell size in each given section were calculated using Infinity capture 6.0 and Image Proplus 5.1 software according to the method reported previously (Yang et al., 2013). All measurements were made on three sites of each tissue, for three sections from each fruit.

Phylogenetic Analysis

Multiple sequence alignment of the C3HC4 domain and typical Ankyrin repeat domain sequences, which were obtained by hidden Markov models corresponding to PF13920 and PF12796 (Gene ID shown in Supplemental Table 2), was performed using the Muscle program with default parameters (Edgar, 2004). The sequence alignments were used for the subsequent phylogenetic analysis. Phylogenetic trees were generated with MEGA7.0 software (https://megasoftware.net/) using the neighbor join algorithms, and the reliability of the obtained trees was assessed with a bootstrap value of 1000.

The evolutionary history was inferred using the Neighbor-Joining method. The bootstrap consensus tree inferred from 1000 replicates is taken to represent the evolutionary history of the taxa analyzed. Branches corresponding to partitions reproduced in less than 50% bootstrap replicates are collapsed. The percentage of replicate trees in which the associated taxa clustered together in the bootstrap test (1000 replicates) are shown next to the branches. The evolutionary distances were computed using the Jones-Taylor-Thornton matrix-based method and are in the units of the number of amino acid substitutions per site. The analysis involved 58 amino acid sequences. All positions containing gaps and missing data were eliminated. There were a total of 202 positions in the final data set. Evolutionary analyses were conducted in MEGA7.

Plasmid Construction and Plant Transformation

The binary vector pBSE402, which contained a CRISPR cassette with a functional Cas9 under a constitutive promoter (*Cauliflower mosaicvirus* 35S) plus a 35S-GFP expression cassette, was modified from pBSE401 (a gift from Qi-Jun Chen). To gain CRISPR/Cas9 engineering mutation in *SF1* gene and *ACS2* gene, single guide RNA (sgRNA) target sites from the N termini of *SF1* and *ACS2* were selected. The sgRNA were assembled into pBSE402 as previously described (Xing et al., 2014). Equal volumes of 100 μM forward and reverse primers were incubated at 95°C for 5 min, and

slowly cooled to room temperature to form a double stranded DNA fragment. This short DNA fragment was then assembled into pBSE402 with BsaI and T4 Ligase (New England Biolabs). Primers are shown in Supplemental Table 3. The final binary vector pBSE402-sgRNA-SF1 and pBSE402-sgRNA-ACS2 were then transformed into Agrobacterium (*Agrobacterium tumefaciens*) strain EHA105.

Agrobacterium-mediated method was used to transform cotyledonary nodes of cucumber as previously described (Hu et al., 2017). CU2 seeds were soaked in distilled water at 50°C for 30 min. Seed coats were removed with forceps and sterilized in 75% (v/v) ethanol for 15 s and 0.6% (v/v) sodium hypochlorite solution for 15 min. The sterilized seeds were germinated in the dark overnight at 28°C in a plastic Petri dish containing 1×Murashige and Skoog medium (Phytotech) supplemented with 2 mg/L 6-benzylaminopurine (Sigma Aldrich) and 1 mg/L abscisic acid (Phytotech). Cotyledons were excised from germination seedlings and infected with Agrobacterium. Subsequently, after shoot regeneration, elongation, and rooting processes, the rooted plants were transplanted to greenhouse.

Genomic DNA was extracted with the DNeasy Plant Mini Kit (Qiagen). The target gene was respectively amplified with specific primers (Supplemental Table 3). PCR products were cloned into pEASY-Blunt Zero (TRANSGEN BIOTECH) and sequenced.

Construction of Near-Isogenic Lines

A series of BC_2S_1 lines were developed using 1983H (*acs2*) as donor and line 406 as recurrent parent (*sf1* and wild type, each for once). The BC_2 population were screened by whole cucumber genome chip containing 181 loci for SNPs test. We chose a BC_2 line whose genotype was heterozygous for both *acs2* and *sf1*; backgrounds were most similar to line 406 and then self-crossed to identify *M E* (wild type), *m E*, *m e*, and *M e* genotypes in a BC_2S_1 population with 500 plants. These plants were used for phenotypic analyses.

Recombinant Protein Expression and Purification

Recombinant proteins GST-SF1, GST-SF1^{R230K}, GST-E2, His-E2, His-SF1, His-SF1^{R230K}, and His-MYC-ACS2 were expressed in BL21 (DE3; TransGen). After induction with 1 mM isopropyl B-D-1-thiogalactopyranoside, cells were harvested and subsequently sonicated in the lysis buffer. The soluble proteins were affinity-purified using Ni-nitrilotriacetic acid Resin (Thermo Fisher Scientific) and Glutathione-Sepharose resin (GE) according to the manufacturer's instructions. Purified supernatant was analyzed by 10% (w/v) SDS-PAGE.

Immunoblotting

SF1 and ACS2 antibodies were produced in rabbit (Agrisera) with synthetic peptides, which matched amino acids 344 to 360 in the SF1 sequence, and 11 to 27 in the ACS2 sequence. The antibody specificity was identified in vitro and in vivo.

Protein extracts of plant tissues were prepared using protein extraction buffer (20 mM Tris-HCl [pH 7.5], 150 mM NaCl, 4 M Urea, 10% (v/v) glycerol, 5 mM DTT, 1 mM phenylmethylsulfonyl fluoride and 1× protease inhibitor cocktail), followed by centrifugation at 12,000g for 30 min at 4°C. Then, 50-100 μg of supernatant was used for 10% (w/v) SDS-PAGE and subsequently transferred to a polyvinylidene fluoride membrane. Immunoblotting signal was visualized using a SuperSignal West Femto kit (Thermo Fisher Scientific).

In Vitro Ubiquitination Assay

Ubiquitin was from BostonBiochem (5 mg, reconstitute at 10 mg/mL in a solution). Yeast GST-E1 was also from BostonBiochem (0.71 mg/mL). Recombinat His-E2 (CsUBC8, the AtUBC8 homologs), His- or GST-SF1, His- or GST-SF1^{R230K}, and His-MYC-ACS2 proteins were purified from *Escherichia coli*, and dialyzed into buffer containing 20 mM Tris-HCl (pH 7.4), 200 mM NaCl, 5% (v/v) glycerol, 1 mM DTT, and 1 mM EDTA. In vitro ubiquitination assays were performed as follows. Each reaction (15 μL volume) contained 5 μg of ubiquitin, 50 ng of recombinant E1, 110 ng E2, and 300 ng purified His-SF1 in ubiquitination buffer (50 mM Tris-HCl [pH 7.4], 5 mM $MgCl_2$, 50 mM KCl, 2 mM ATP, and 1 mM DTT). After incubation at 30°C for 2 h, the reaction was stopped by adding 5 × SDS sample buffer, and analyzed by electrophoresis on 12% (w/v) SDS gels. Ubiquitinated SF1 or ACS2 was detected using anti-ubiquitin antibody or anti-His antibody.

In Vivo Ubiquitination Assay

In vivo ubiquitination assay was performed according to the protocol described by Liu et al. (Liu et al., 2010). We coinfiltrated the agrobacteria carrying the FLAG-ACS2 and MYC-SF1 plasmids into tobacco leaves, and the corresponding empty vectors were used as the controls. To keep the consistence in all loading sample, the agrobacteria carrying 35S-GFP was used as an internal control. For inhibition of 26S-proteasome, 50 mM MG132 (Sigma-Aldrich; in 10 mM $MgCl_2$ solution) was infiltrated 12 h before leave collection. Samples were collected for protein and RNA extraction after 3 d. For protein analysis, the extracts were analyzed using anti-FLAG, anti-MYC and anti-GFP antibodies (Supplemental Table 4). For RNA level expression analysis, RT-PCR was performed.

GST-Pull Down

The pull-down assay was conducted as previously described with some modifications (Oh et al., 2012). In brief, 2 μg of GST-SF1, GST-SF1^{R230K}, or GST bound glutathione agarose beads were incubated with 2 μg of His-MYC-ACS2 in 1× PBS buffer (137 mM NaCl, 2.7 mM KCl, 10 mM Na_2HPO_4, 2 mM KH_2PO_4, pH7.4) at 4°C on a platform that swings up and down for 1 h. After being washed three times with 1× PBS buffer, the beads were directly added with an equal volume of 1× SDS sample buffer and w detected by immunoblotting using anti-MYC antibody.

Yeast Two-Hybrid Assays

Yeast two-hybrid assays were performed using the GAL4-based Two-Hybrid System (Clontech), according to the manufacturer's instructions. The full-length cDNA of SF1, SF1^{R230K}, and ACS2 were subcloned into the pGADT7 and pGBKT7 vectors, respectively. Yeast (*Saccharomyces cerevisiae*) strain AH109 was used for transformation, and then was grown in 2D (SD-Leu-Trp) medium. The transformed colonies were plated onto a 4D (SD-Ade-Leu-Trp-His) medium plates to verify the interaction. The primers used for yeast two-hybrid assays are listed in Supplemental Table 3.

Coimmunoprecipitation

Cultured Agrobacteria harboring pCAMBIA1300-FLAG-ACS2, pCAMBIA1300-MYC-SF1, or pCAMBIA1300-MYC-SF1^{R230K} and P19 were resuspended in 10 mM MES (pH 5.8) buffer containing 10 mM $MgCl_2$ and 200 μM acetosyringone at a ratio of 1:1:2. After 2 h incubation at room temperature in darkness, the strains were infiltrated into healthy and fully expanded leaves of 4-week-old *N. benthamiana* plants using a needleless syringe. The infiltrated leaves were harvested after 2 d, and total protein was extracted in IP buffer (25 mM Tris-HCl [pH 7.4], 150 mM NaCl, 1% (v/v) Nonidet P-40, 5% (v/v) glycerol, 1 mM DTT, 1 mM phenylmethylsulfonyl fluoride, and protease inhibitor cocktail). The extracted protein was incubated with anti-MYC agarose conjugates (Sigma Aldrich) for 2 h at 4°C. The beads were then washed three times with washing buffer (150 mM NaCl, 5 mM EDTA, and 50 mM Tris-HCl [pH 7.5]), and beads were sampled for

coimmunoprecipitation analysis. Anti-MYC antibody and anti-FLAG antibody (Sigma Aldrich) were used for immunoblots (Supplemental Table 4).

RNA Seq Analysis

Total RNA was extracted from 0 DAA fruits of wild type (*M E*), *m e*, *m E*, and *M e* plants with two biological replications using a TRIzol kit (Invitrogen) according to the protocol. Sequencing cDNA libraries with an average insert size of 250-300 bp were prepared according to the manufacturer's instructions (Illumina), and 150-bp paired-end reads were generated on an Illumina Hiseq 2000 Analyzer. The fragments per kilobase of transcript per million mapped reads expression value of each gene was calculated using StringTie (Pertea et al., 2016). Genes with a fold change >1.5 or <0.67, and a *p* value of < 0.05 in the *t* test (one-tailed) were defined as differentially expressed genes.

RT-quantitative PCR Analysis

Total RNA was extracted using TRIzol reagent (Invitrogen). First-strand cDNA was synthesized using 1 μg total RNA with the Moloney Murine Leukemia VirusReverse Transcriptase (Promega), and then a quantitative PCR assay was performed on an ABI 7900 (Applied Biosystems) machine using SYBR Premix (Roche) according to the manufacturer's instructions. Three independent biological replicates were performed. Relative gene expression was performed using the $2^{-\Delta\Delta Ct}$ method. The *UBIQUITIN* gene, *Csa3G778350,* was used as an internal reference gene. Primers are listed in Supplemental Table 3.

Exogenous Ethylene Treatment

One-month-old wild-type (1983G) and *acs2* (1983H) cucumber plants were placed in four acrylic chambers, with five plants of wild type and five plants of *acs2* in a chamber. The side of each chamber was sealed with a rubber stopper that formed a gas inlet/outlet to facilitate the injection of the ethylene gas. The ethylene source was a pressurized gas tank containing a known concentration of ethylene gas. Plants were provided with normal water and fertilizer. The concentrations of ethylene in chambers were determined using the known concentration of ethylene stock and the chamber volume (1 m^3). The four chambers are individually treated with different concentrations of ethylene at 0, 10^{-1}, 10°, and 10^1 ppm for 1 week. Ethylene gas was changed with fresh air twice a day, for 30 min each time. The fruits from 11 and 12 nodes were used for phenotype observation. Half of the fruits were used for data collection at 0 DAA, and half were allowed to grow for data collection at 16 DAA.

Ethylene Measurement

The 0 DAA fruits of wild type (1983G) and *acs2* (1983H), wild type (406) and *sf1*, and wild type (*M E*), *m e*, *m E*, and *M e* plants were excised to measure the ethylene release. At least three biological replicates were measured. Each sample was placed in a 65-mL container with a piece of wet cotton at the bottom and sealed with a rubber stopper. After incubation at 23°C for 1 h, the containers were opened to volatilize the ethylene induced by cutting. Samples were incubated in a sealed container at 23°C for another 10 h in the dark, and 10 μL of gas was removed with a syringe and injected into a gas chromatograph (Agilent 7890B-5977A) equipped with a flame-ionization detector and a capillary column for ethylene measurements. All determinations were made in triplicate. The ethylene release rate (nanoliliters per gram fresh weight per hour) was calculated on the basis of fresh weight of fruits.

Statistical Analyses

In the case of comparisons between two sample groups, the Student's *t* test was applied. For multiple comparison, significance analysis was performed as pairwise comparison based on ANOVA, which was followed by Tukey's honestly significant difference test and was performed in R for statistical evaluation (Supplemental Data Set 4).

Data Availability

All data that support the findings within this article are available from the corresponding author upon reasonable request.

Accession Numbers

Sequence data from this article can be found in the Cucurbit Genomics Database (www.icugi.org) under accession numbers SF1(Csa2G174140); ACS2(Csa1G580750); and CsUBC8 (Csa6G133760).

Supplemental Data

Supplemental Figure 1. Morphological and physiological changes of WT and *sf1* cucumber fruit during early development.

Supplemental Figure 2. Identification and phenotypic analysis of CRISPR-SF1 plants.

Supplemental Figure 3. mRNA and protein expression profiles of SF1 in various cucumber tissues.

Supplemental Figure 4. Purification of recombinant proteins for biochemical assays.

Supplemental Figure 5. Treatment with 1-MCP showed dose effects on sf1 fruit elongation.

Supplemental Figure 6. 1-MCP treatment partially complemented the short fruit phenotype of sf1.

Supplemental Figure 7. *ACS2* knock-out cucumber plants displayed androecy.

Supplemental Figure 8. mRNA and protein expression profiles of *ACS2* in various cucumber tissues.

Supplemental Figure 9. Proteasome-dependent degradation of ACS2.

Supplemental Figure 10. Fruit ontology of WT (*M E*), *m e*, *m E*, and *M e* during early development stages.

Supplemental Figure 11. Cell size difference in fruits between WT and *acs2* along transversal axis.

Supplemental Table 1. Phenotypic statistics of selfed F2.

Supplemental Table 2. The gene ID for phylogenetic tree analysis.

Supplemental Table 3. Primers used in this study.

Supplemental Table 4. Antibodies used in this study.

Supplemental Data Set 1. The SNP-index from MutMap analysis.

Supplemental Data Set 2. Alignment of genes used to generate the phylogeny shown in Figure 1K.

Supplemental Data Set 3. Differential expression of genes in fruit cells at 0 DAA in sf1 mutants and WT ($P < 0.05$).

Supplemental Data Set 4. ANOVA and *t* test.

ACKNOWLEDGMENTS

We thank Qi Xie from Chinese Academy of Sciences and Juan Xu from Zhejiang University for comments on the article. We also thank Jingjin Sun and Yuanchao Xu for experimental assistance from Institute of Vegetables

and Flowers, Chinese Academy of Agricultural Sciences. This work was supported by grants from the National Natural Science Foundation of China (NSFC) (grants 31530066 to S.H., 313220419 to Z.H.Z., and 31572117 to X.Y.) and the National key R&D Program of China (2016YFD0101007 and 2016YFD0100500). Additional support was provided by ASTIP-CAAS (CAAS-XTCX2016001), the Leading Talents of Guangdong Province Program (grant 00201515 to S.H.), and the Shenzhen Municipal, The Peacock Plan (KQTD2016113010482651) and the Dapeng district government.

AUTHOR CONTRIBUTIONS

T.X., Z.Z., and X.Y. made major contributions to biochemical assays and interpreted the data and wrote the article; T.X. and X.Y. led genetic transformation of plants; Z.Z., S.L., S.Z., and X.Y. performed the mutant screen, genetic studies, and phenotype observations; Q.L., Z.H.Z., and X.Y. led bioinformatic analyses; S.H. and X.Y. designed the research.

Received January 2, 2019; revised March 5, 2019; accepted March 20, 2019; published March 26, 2019.

REFERENCES

Adams, D.O., and Yang, S.F. (1979). Ethylene biosynthesis: Identification of 1-aminocyclopropane-1-carboxylic acid as an intermediate in the conversion of methionine to ethylene. Proc. Natl. Acad. Sci. USA **76:** 170–174.

Bisognin, D.A. (2002). Origin and evolution of cultivated cucurbits. Cienc. Rural **32:** 715–723.

Bo, K., Ma, Z., Chen, J., and Weng, Y. (2015). Molecular mapping reveals structural rearrangements and quantitative trait loci underlying traits with local adaptation in semi-wild Xishuangbanna cucumber (*Cucumis sativus* L. *var. xishuangbannanesis* Qi et Yuan). Theor. Appl. Genet. **128:** 25–39.

Boualem, A., Troadec, C., Camps, C., Lemhemdi, A., Morin, H., Sari, M.-A., Fraenkel-Zagouri, R., Kovalski, I., Dogimont, C., Perl-Treves, R., and Bendahmane, A. (2015). A cucurbit androecy gene reveals how unisexual flowers develop and dioecy emerges. Science **350:** 688–691.

Chen, H., et al. (2016). An ACC oxidase gene essential for cucumber carpel development. Mol. Plant **9:** 1315–1327.

Colle, M., Weng, Y., Kang, Y., Ophir, R., Sherman, A., and Grumet, R. (2017). Variation in cucumber (*Cucumis sativus* L.) fruit size and shape results from multiple components acting pre-anthesis and post-pollination. Planta **246:** 641–658.

De Grauwe, L., Vandenbussche, F., Tietz, O., Palme, K., and Van Der Straeten, D. (2005). Auxin, ethylene and brassinosteroids: Tripartite control of growth in the *Arabidopsis* hypocotyl. Plant Cell Physiol. **46:** 827–836.

Dugardeyn, J., and Van Der Straeten, D. (2008). Ethylene: Fine-tuning plant growth and development by stimulation and inhibition of elongation. Plant Sci. **175:** 59–70.

Edgar, R.C. (2004). MUSCLE: Multiple sequence alignment with high accuracy and high throughput. Nucleic Acids Res. **32:** 1792–1797.

Grumet, R., and Colle, M. (2016). Genomic analysis of cucurbit fruit growth. In R Grumet, N Katzir, and J Garcia-Mas, eds, Genetics and Genomics of Cucurbitaceae. Plant Genetics and Genomics: Crops and Models. Springer, Cham, pp 321–344.

Guzmán, P., and Ecker, J.R. (1990). Exploiting the triple response of *Arabidopsis* to identify ethylene-related mutants. Plant Cell **2:** 513–523.

Hu, B., Li, D., Liu, X., Qi, J., Gao, D., Zhao, S., Huang, S., Sun, J., and Yang, L. (2017). Engineering non-transgenic gynoecious cucumber using an improved transformation protocol and optimized CRISPR/Cas9 system. Mol. Plant **10:** 1575–1578.

Kazama, H., Dan, H., Imaseki, H., and Wasteneys, G.O. (2004). Transient exposure to ethylene stimulates cell division and alters the fate and polarity of hypocotyl epidermal cells. Plant Physiol. **134:** 1614–1623.

Kieber, J.J., Rothenberg, M., Roman, G., Feldmann, K.A., and Ecker, J.R. (1993). CTR1, a negative regulator of the ethylene response pathway in *Arabidopsis*, encodes a member of the raf family of protein kinases. Cell **72:** 427–441.

Le, J., Vandenbussche, F., De Cnodder, T., Van Der Straeten, D., and Verbelen, J.-P. (2005). Cell elongation and microtubule behavior in the *Arabidopsis* hypocotyl: Responses to ethylene and auxin. J. Plant Growth Regul. **24:** 166–178.

Li, Z., et al. (2009). Molecular isolation of the M gene suggests that a conserved-residue conversion induces the formation of bisexual flowers in cucumber plants. Genetics **182:** 1381–1385.

Li, Z., Wang, S., Tao, Q., Pan, J., Si, L., Gong, Z., and Cai, R. (2012). A putative positive feedback regulation mechanism in CsACS2 expression suggests a modified model for sex determination in cucumber (*Cucumis sativus* L.). J. Exp. Bot. **63:** 4475–4484.

Liu, L., Zhang, Y., Tang, S., Zhao, Q., Zhang, Z., Zhang, H., Dong, L., Guo, H., and Xie, Q. (2010). An efficient system to detect protein ubiquitination by agroinfiltration in *Nicotiana benthamiana.* Plant J. **61:** 893–903.

Liu, S., Xu, L., Jia, Z., Xu, Y., Yang, Q., Fei, Z., Lu, X., Chen, H., and Huang, S. (2008). Genetic association of ETHYLENE-INSENSITIVE3-like sequence with the sex-determining M locus in cucumber (*Cucumis sativus* L.). Theor. Appl. Genet. **117:** 927–933.

Lyzenga, W.J., Booth, J.K., and Stone, S.L. (2012). The *Arabidopsis* RING-type E3 ligase XBAT32 mediates the proteasomal degradation of the ethylene biosynthetic enzyme, 1-aminocyclopropane-1-carboxylate synthase 7. Plant J. **71:** 23–34.

Martínez, C., Manzano, S., Megías, Z., Garrido, D., Picó, B., and Jamilena, M. (2013). Involvement of ethylene biosynthesis and signalling in fruit set and early fruit development in zucchini squash (*Cucurbita pepo* L.). BMC Plant Biol. **13:** 139.

Monforte, A.J., Diaz, A., Caño-Delgado, A., and van der Knaap, E. (2014). The genetic basis of fruit morphology in horticultural crops: Lessons from tomato and melon. J. Exp. Bot. **65:** 4625–4637.

Neff, M.M., Neff, J.D., Chory, J., and Pepper, A.E. (1998). dCAPS, a simple technique for the genetic analysis of single nucleotide polymorphisms: experimental applications in *Arabidopsis thaliana* genetics. Plant J. **14:** 387–392.

Nodzon, L.A., Xu, W.H., Wang, Y., Pi, L.Y., Chakrabarty, P.K., and Song, W.Y. (2004). The ubiquitin ligase XBAT32 regulates lateral root development in *Arabidopsis.* Plant J. **40:** 996–1006.

Oh, E., Zhu, J.-Y., and Wang, Z.-Y. (2012). Interaction between BZR1 and PIF4 integrates brassinosteroid and environmental responses. Nat. Cell Biol. **14:** 802–809.

Ortega-Martínez, O., Pernas, M., Carol, R.J., and Dolan, L. (2007). Ethylene modulates stem cell division in the *Arabidopsis thaliana* root. Science **317:** 507–510.

Pan, Y., Liang, X., Gao, M., Liu, H., Meng, H., Weng, Y., and Cheng, Z. (2017). Round fruit shape in WI7239 cucumber is controlled by two interacting quantitative trait loci with one putatively encoding a tomato SUN homolog. Theor. Appl. Genet. **130:** 573–586.

Pertea, M., Kim, D., Pertea, G.M., Leek, J.T., and Salzberg, S.L. (2016). Transcript-level expression analysis of RNA-seq experiments with HISAT, StringTie and Ballgown. Nat. Protoc. **11:** 1650–1667.

Pierik, R., Visser, E.J., de Kroon, H., and Voesenek, L.A. (2003). Ethylene is required in tobacco to successfully compete with proximate neighbours. Plant Cell Environ. **26:** 1229–1234.

Pierik, R., Cuppens, M.L., Voesenek, L.A., and Visser, E.J. (2004). Interactions between ethylene and gibberellins in phytochrome-mediated shade avoidance responses in tobacco. Plant Physiol. **136:** 2928–2936.

Pierik, R., Tholen, D., Poorter, H., Visser, E.J.W., and Voesenek, L.A.C.J. (2006). The Janus face of ethylene: Growth inhibition and stimulation. Trends Plant Sci. **11:** 176–183.

Prasad, M.E., Schofield, A., Lyzenga, W., Liu, H., and Stone, S.L. (2010). *Arabidopsis* RING E3 ligase XBAT32 regulates lateral root production through its role in ethylene biosynthesis. Plant Physiol. **153:** 1587–1596.

Qi, J., et al. (2013). A genomic variation map provides insights into the genetic basis of cucumber domestication and diversity. Nat. Genet. **45:** 1510–1515.

Rudich, J., Halevy, A.H., and Kedar, N. (1969). Increase in femaleness of three cucurbits by treatment with Ethrel, an ethylene releasing compound. Planta **86:** 69–76.

Saibo, N.J.M., Vriezen, W.H., Beemster, G.T.S., and Van Der Straeten, D. (2003). Growth and stomata development of *Arabidopsis* hypocotyls are controlled by gibberellins and modulated by ethylene and auxins. Plant J. **33:** 989–1000.

Shinozaki, Y., et al. (2015). Ethylene suppresses tomato (*Solanum lycopersicum*) fruit set through modification of gibberellin metabolism. Plant J. **83:** 237–251.

Smalle, J., Haegman, M., Kurepa, J., Van Montagu, M., and Straeten, D.V. (1997). Ethylene can stimulate *Arabidopsis* hypocotyl elongation in the light. Proc. Natl. Acad. Sci. USA **94:** 2756–2761.

Vandenbussche, F., et al. (2003). The *Arabidopsis* mutant alh1 illustrates a cross talk between ethylene and auxin. Plant Physiol. **131:** 1228–1238.

Vandenbussche, F., Vaseva, I., Vissenberg, K., and Van Der Straeten, D. (2012). Ethylene in vegetative development: A tale with a riddle. New Phytol. **194:** 895–909.

Wang, K.L.C., Yoshida, H., Lurin, C., and Ecker, J.R. (2004). Regulation of ethylene gas biosynthesis by the *Arabidopsis* ETO1 protein. Nature **428:** 945–950.

Wei, Q., Wang, Y., Qin, X., Zhang, Y., Zhang, Z., Wang, J., Li, J., Lou, Q., and Chen, J. (2014). An SNP-based saturated genetic map and QTL analysis of fruit-related traits in cucumber using specific-length amplified fragment (SLAF) sequencing. BMC Genomics **15:** 1158.

Wen, C.-K. (2014). Ethylene in Plants. Springer, Netherlands.

Weng, Y., Colle, M., Wang, Y., Yang, L., Rubinstein, M., Sherman, A., Ophir, R., and Grumet, R. (2015). QTL mapping in multiple populations and development stages reveals dynamic quantitative trait loci for fruit size in cucumbers of different market classes. Theor. Appl. Genet. **128:** 1747–1763.

Xing, H.-L., Dong, L., Wang, Z.-P., Zhang, H.-Y., Han, C.-Y., Liu, B., Wang, X.-C., and Chen, Q.-J. (2014). A CRISPR/Cas9 toolkit for multiplex genome editing in plants. BMC Plant Biol. **14:** 327.

Yang, S.F., and Hoffman, N.E. (1984). Ethylene biosynthesis and its regulation in higher plants. Annu. Rev. Plant Physiol. **35:** 155–189.

Yang, X.Y., Wang, Y., Jiang, W.J., Liu, X.L., Zhang, X.M., Yu, H.J., Huang, S.W., and Liu, G.Q. (2013). Characterization and expression profiling of cucumber kinesin genes during early fruit development: Revealing the roles of kinesins in exponential cell production and enlargement in cucumber fruit. J. Exp. Bot. **64:** 4541–4557.

Zhang, W., and Wen, C.-K. (2010). Preparation of ethylene gas and comparison of ethylene responses induced by ethylene, ACC, and ethephon. Plant Physiol. Biochem. **48:** 45–53.